

ANN-based performance estimation of a slotted inverted F-shaped tri-band antenna for satellite/mm-wave 5G application

Md. Kawsar Ahmed¹, Kamal Hossain Nahin¹, Md. Sharif Ahammed¹, Md. Ashraful Haque¹, Narinderjit Singh Sawaran Singh², Redwan Al Mahmud Asad Ananta¹, Jamal Hossain Nirob¹, Mirajul Islam³, Liton Chandra Paul⁴

¹Department of Electrical and Electronic Engineering, Daffodil International University, Dhaka, Bangladesh

²Faculty of Data Science and Information Technology, INTI International University, Nilai, Malaysia

³Department of Computer Science and Engineering, Daffodil International University, Dhaka, Bangladesh

⁴Department of Electrical, Electronic, and Communication Engineering, Pabna University of Science and Technology, Pabna, Bangladesh

Article Info

Article history:

Received Feb 1, 2024

Revised Mar 12, 2024

Accepted Mar 29, 2024

Keywords:

5G

Antenna

Artificial neural network

Industrial and innovation

Satellite

Tri-band

ABSTRACT

In this research, we explain comprehensive industrial and innovation results on using an artificial neural network (ANN) method to improve the performance of microstrip patch antennas for 5G, indoor-outdoor, and Ku band uses. To determine if an antenna is appropriate, this article discusses multiple methods, one of which is to do a simulation using validating software like high frequency structure simulator (HFSS) and Altair Feko. Based on the Rogers RT 5880 substrate, the antenna is constructed. There is a loss tangent of 0.0009 and its dimensions are 17.1053 mm in length and 16 mm in width. Its dielectric constant is 2.2. Despite its small size, it boasts an impressive maximum efficiency of almost 90% and a gain of approximately 8 dB. As an indicator of ANN model performance, we may look at the R-squared value (99%), the mean square error (MSE), which is approximately 0.0015, and the confidence interval (99%). The ANN models are the most accurate and have the lowest error rate when it comes to predicting efficiency and gain. The suggested antenna is a promising contender for the targeted Ku band, indoor/outdoor, and 5G uses, as verified by the clustering of computer simulation technology (CST), HFSS, and Altair Feko simulated results with the measured and predicted outcomes of ANN approach.

This is an open access article under the [CC BY-SA](#) license.



Corresponding Author:

Narinderjit Singh Sawaran Singh

Faculty of Data Science and Information Technology, INTI International University

Persiaran Perdana BBN, Putra Nilai, Nilai 71800, Negeri Sembilan, Malaysia

Email: narinderjits.sawaran@newinti.edu.my

1. INTRODUCTION

Wireless cellular networks have become an essential component of day-to-day life, as they offer pervasive mobile communication services and make it possible for a wide variety of applications that go beyond voice and text, including mobile internet, video calling, and connectivity for the internet of things devices [1]. Ku-band is a portion of the electromagnetic (EM) spectrum commonly used for various applications, particularly in the field of telecommunications and satellite communications. The Ku-band spans a frequency range from approximately 12 to 18 gigahertz (GHz) [2]. Ku-band has some advantages over lower frequency bands like C and X bands [3], including faster data rates and relatively excellent resistance to rain attenuation, although it may be more vulnerable to signal deterioration in severe weather circumstances. The millimeter wave (mm-wave) spectrum includes frequencies in the 20-25 GHz range. The higher frequency bands are

useful for both indoor and outdoor use, especially for short-range, high-capacity wireless communication [4]. There are some distinct features of mm-wave frequencies like 20–25 GHz. They have a shorter effective range than lower-frequency bands and are easily disrupted by physical barriers, but they provide a high data throughput [5]. That's why it's important to think about things like line-of-sight, route loss, and signal obstruction from buildings and foliage before putting them into use. The 28 GHz band is an important one for 5G networks in some areas because it is part of the mm-wave spectrum [6]. High data rates and minimal latency are only two of the many advantages of using the 28 GHz spectrum in 5G applications. It's worth noting that spectrum allocation and regulatory decisions can affect whether the 28 GHz band is made available for 5G in each region or country [7]. The limited propagation properties of mm-wave frequencies necessitate meticulous planning and infrastructure implementation for 28 GHz 5G networks. This technology works in tandem with 5G bands operating at lower frequencies to improve coverage and penetration through obstructions [8]. Microstrip patch antennas are a popular choice for radio frequencies (RF) and microwave applications in wireless communication systems. Its small size and flat profile make it a good fit for incorporation into a wide range of electrical gadgets, including mobile phones, Wi-Fi access points, and even radar systems [9].

This study aims to conduct a simulation and performance analysis of a microstrip patch antenna utilizing computer simulation technology (CST) EM simulation tools. The validation of CST simulation findings, including the reflection coefficient, gain, and efficiency, is conducted through the utilization of Altair Feko simulation software and high frequency structure simulator (HFSS). The simulated outcomes are subsequently compared. In recent times, there has been an exploration of a novel approach including the utilization of artificial neural network (ANN) techniques to predict efficiency and gain through the application of CST EM modeling tools. Conceptually, Table 1 compares several current projects. In the works [10]–[15], the suggested antenna has been said to have gains of 6.5 dB, 5.8 dB, 4.6 dB, 7.4 dB, 6.08 dB, and 8.3 dB. However, the gain that was seen in CST is 8.5 dB. CST says that the suggested architecture has a bandwidth of 2.34 GHz in the first band, 4.369 GHz in the second band, and 3.614 GHz in the third band. The reports talked about 3 GHz, 1.1 GHz, 0.51 GHz, 1.09 GHz, and 4.1 GHz as bandwidths. It is suggested that the antenna has a radiation rate of 96.27%, which is higher than the 90%, 80%, 80.8%, and 82% found in the studies [10], [12], [14], [15]. While the table's list of references did not make use of ANN, the stated investigation does extensively rely on ANN.

Table 1. Performance comparison with related works

Reference	Frequency	Return loss	Bandwidth (BW)	Size (mm ²)	Peak gain	Maximum efficiency (%)	Substrate	ANN investigation
[10]	28	-30	3	30×30	6.5	90	Roger RT 5880	No
[11]	12.85	-23	-	31.16×27.04	5.8	-	Roger RT 5880	No
[12]	5, 11.5, 14.1	-20.9, -36.2, -40.9	0.7, 1.1, 1.1	50×40	4.6	80	Roger RT 5880	No
[13]	12.24	-16	0.51	0.92 λ_0 ×0.90 λ_0	7.4	-	F4BME220	No
[14]	11.79, 15.77	-25, -37	1.09, 0.83	30× 13	6.08	80.8	Arlon DiClad 880	No
[15]	28	-30	4.1	30×35×0.76	8.3	82	Rogers RO4350B	No
Proposed	17.549, 21.56, 27.965	-23.85, -30.82, -29.47	2.34, 4.369, 3.614	17.10×16	8.5	96.27	Rogers RT 5880	Yes

2. DESIGN METHOD

Figure 1 displays the intricate structure of the microstrip patch antenna that has been suggested. The antenna is fabricated on a 20×20 mm² Rogers RT 5880 substrate with a dielectric constant of 2.2 and a loss tangent of 0.0009. The substrate has a height or thickness of 1.5 mm. The initial idea involved creating a patch, a feedline, and a ground that was totally covered [16]. The radiating section is 17.1053×16 mm² and is connected to a feedline of 3.6×4.5 mm². We enhanced the antenna performance by adding slots and creating a partial ground, which altered the current distribution within the antenna and thus impacted the findings [17]. A rectangular slot measuring 8×5 mm² is created on the left side of the patch. The slot starts 2.70 mm below the top left corner of the patch. A circular slot with a radius of $r = 1$ mm is added to the upper right corner of the patch and is positioned 4 mm to the left and 3.75 mm down from the top right corner of the patch. The ground was finally reduced slightly on the top, as well as on both the right and left sides. The ground dimension measures 18×8 mm². HFSS, CST, and Altair Feko were utilized to simulate the proposed antenna to validate the accuracy of our simulated outcome. Table 2 displays the accurate and revised physical dimensions of the proposed antenna.

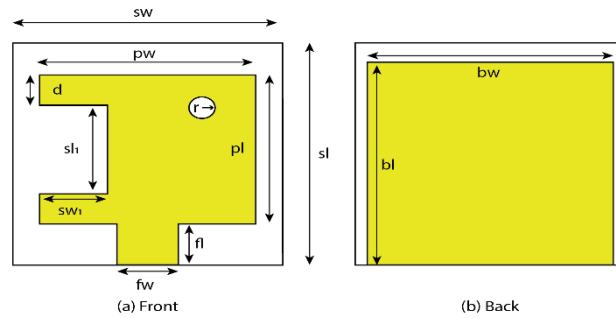


Figure 1. Structure of the proposed antenna

Table 2. Design parameters of the antenna structure

SL. No.	Parameter	Symbol	Size (mm)	SL.No.	Parameter	Symbol	Size (mm)
01	Length of patch	pl	17.1053	08	Length of feed line	fl	3.6
02	Width of patch	pw	16	09	Width of feed line	fw	4.5
03	Patch thickness	t	0.035	10	Slot width	Swl	5
04	Length of substrate	sl	20	11	Slot length	S11	8
05	Width of substrate	sw	20	12	Radius	r	1
06	Substrate thickness	st	1.5	13	Distance	d	2.70
07	Length of ground plane	bl	18	14	Width of ground plane	bw	08

3. EFFECTS OF CHANGING THE WIDTH AND LENGTH OF THE PATCH AND GROUND PLANE

3.1. Effect of changing ground width

Evaluation of ground plane on antenna’s operational reliability is critical. Resonant frequencies for 18 mm ground plane width are 17.549, 21.56, and 27.965 GHz with reflection coefficients of -23.85, -30.823, and -29.475 dB, respectively. The frequencies and corresponding reflection coefficients change to 17.465 GHz, 21.644 GHz, 28.112 GHz, -19.835 dB, -26.079 dB, and -21.609 dB after increasing the ground width to 1.5789 mm. The frequencies and reflection coefficients for 16.604 GHz, 21.959 GHz, and 28.448 GHz are -26.28 dB, -42.317 dB, and -38.329 dB, respectively, when the ground plane is 2 mm wide. The antenna’s ground plane width affects the simulated reflection coefficient, as seen in Figure 2. Wider ground shifts frequency down the spectrum. Also, the reflection coefficient decreases. However, as ground plane width diminishes, frequency shifts to the higher spectrum. This scenario also increases the reflection coefficient [18].

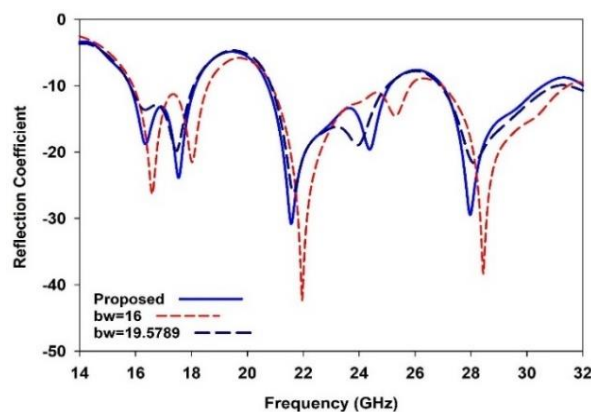


Figure 2. Reflection coefficient response for different widths of ground plane

3.2. Effect of changing patch width

Along with the length of the patch, width of the patch also determines antenna performance. The resonant frequencies are 17.549 GHz, 21.56 GHz, and 27.965 GHz for 16 mm patch width (pw). Their corresponding reflection coefficients are -23.85, -30.823, and -29.475 dB, respectively. After expanding the pw to 16.74 mm, the frequencies and reflection coefficients are 17.255 GHz, 23.618 GHz, 27.713 GHz, -16.481 dB, -34.873 dB,

and -20.485 dB, respectively. With a pw of 14.84 mm, resonant frequencies of 17.465 GHz, 22.169 GHz, and 28.721 GHz and reflection coefficients of -23.573, -29.121, and -28.218 dB were achieved. The antenna pw affects the simulation reflection coefficient, as seen in Figure 3. Increased patch width shifts the frequency to the lower spectrum, decreasing the reflection coefficient [19]. In contrast, reducing the pw to 14.84 mm, it raises the resonant frequency. Additionally, the reflection coefficient also rises.

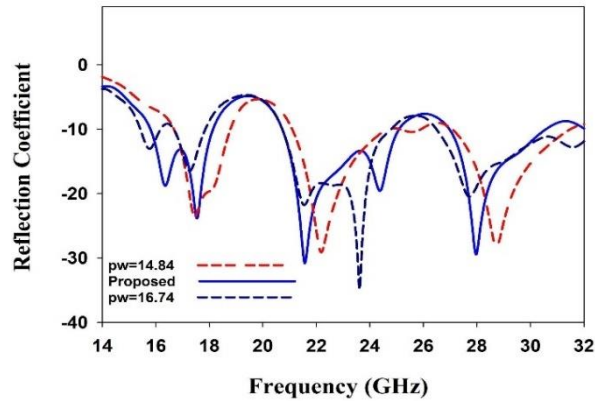


Figure 3. Response of the reflection coefficient for different pw

3.3. Effect of changing patch length

The antenna's performance depends on patch length (pl). Resonant frequencies and reflection coefficients for 17.1053 mm pl are obtained as 17.549, 21.56, and 27.965 GHz and -23.85, -30.823, and -29.475 dB respectively. By adding 1.6842 mm to the pl, the frequency and reflection coefficient are shifted to 17.192 GHz, 21.098 GHz, 26.726 GHz, -20.944 dB, -24.858 dB, and -30.911 dB. The frequencies of 17.759 GHz, 22.001 GHz, and 28.343 GHz are measured at 16.68 mm, together with their reflection coefficients of -19.688, -21.684, and -20.588 dB. As pl increases, frequency changes to lower spectrum [20]. Frequency rises as pl decreases to 16.68 mm. This also lowers the reflection coefficient. The antenna pl affects the simulated reflection coefficient, as seen in Figure 4.

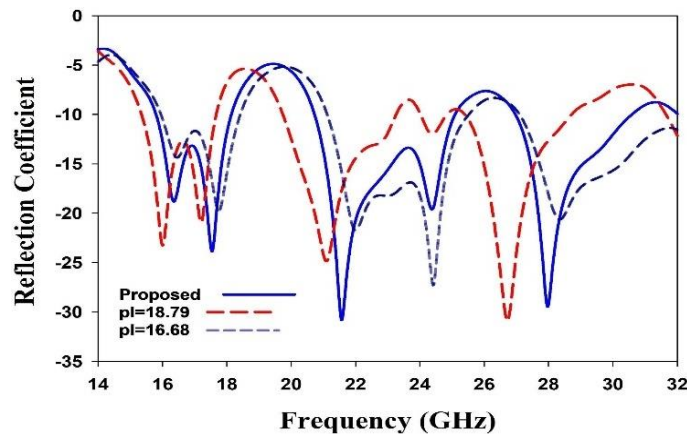


Figure 4. Response of the reflection coefficient for the different pl

4. RESULTS AND DISCUSSION

4.1. Reflection coefficient

The reflection coefficient in patch antennas is strongly linked to return loss and is used to evaluate the impedance mismatch between the antenna and the feeding network [21]. It is generally preferred to achieve a high return loss. Figure 5 illustrates the reflection coefficient of the suggested antenna designed and simulated using CST, HFSS, and Altair Feko software. The results obtained from CST software show that the antenna

exhibits resonances at 17.549 GHz, 21.56 GHz, and 27.965 GHz, with a corresponding return loss of -23.85, -30.825, and -29.475 dB respectively. The antenna exhibits bandwidths of 2.34 GHz (15.799–18.139 GHz), 4.369 GHz (20.724–25.093 GHz), and 3.614 GHz (26.97–30.584 GHz) for these respective frequencies. On the other hand, HFSS simulations reveal resonances at slightly lower frequencies of 17.213 GHz, 21.098 GHz, and 26.789 GHz, accompanied by return losses of -21.674, -24.926, and -31.769 dB respectively. The bandwidths obtained from HFSS are slightly narrower, with 2.286 GHz (15.375–17.661 GHz), 3.521 GHz (19.764–23.285 GHz), and 3.256 GHz (25.446–28.702 GHz) for the corresponding resonant frequencies. In Altair Feko, the antenna exhibits resonances at 18.137, 22.925, and 28.931 GHz, with corresponding reflection coefficients of -22.658, -30.03, and -32.261 dB, resulting in bandwidths of 1.693 GHz (19.003–17.31 GHz), 3.576 GHz (21.402–24.978 GHz), and 4.9 GHz (27.095–32 GHz). The discrepancies might be due to variances in the algorithms and numerical methodologies used by the software programs. Despite the differences, both simulations reveal that the antenna can cover a wide frequency range, which provides flexibility for Ku band applications and applications that take place indoors, outdoors, and with 5G.

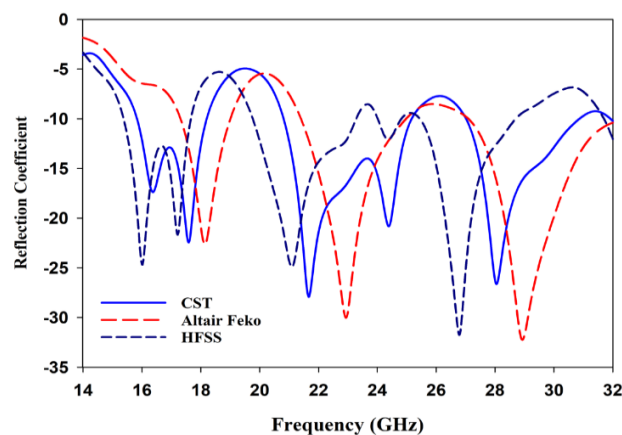


Figure 5. Reflection coefficient of the proposed antenna

4.2. Gain

Gain is critical in patch antennas, indicating their capacity to concentrate and guide emitted energy in a particular direction [22]. Figure 6 illustrates that the highest gain in CST is recorded as 8.547 dB, but the gain at the resonant frequency is 4.9712 dB, 7.4562 dB, and 8.547 dB, respectively. HFSS simulations, on the other hand, produce the highest possible gain of 7.28 dB, with resonant frequencies displaying gains of 4.9339 dB, 7.2601 dB, and 6.1082 dB, respectively. There was also a change in gain that was seen when the Altair Feko software was used to design the antenna. The antenna shows a maximum gain of 8.5 dB, while the gain at the resonant frequency is reported as 6.1276 dB, 7.2671 dB, and 6.9869 dB, respectively. Despite these differences, the antenna displays resonances with strengths that are much higher than average, which suggests that it may be suitable for applications that need adequate signal reception and transmission.

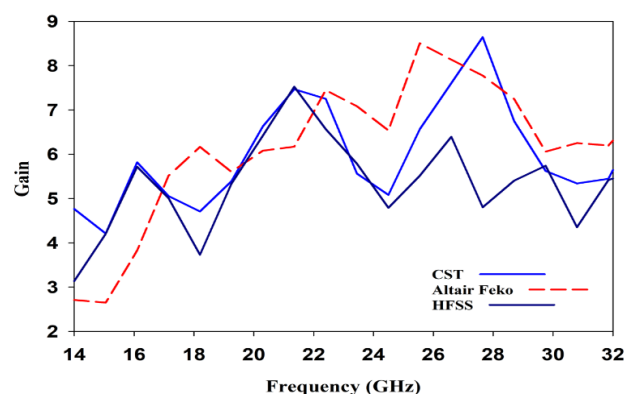


Figure 6. Gain of the proposed antenna

4.3. Efficiency

Efficiency in patch antennas pertains to the antenna's capacity to transform input power into radiated power efficiently [23]. There are considerable differences in the microstrip patch antenna's efficiency, as shown in Figure 7. The highest efficiency achieved in CST simulations is 96.27%, whereas in HFSS simulations, it is somewhat lower at 93.279%. In addition, the highest efficiency was recorded as 97.03% when the antenna was developed using Altair Feko.

However, upon closer inspection, the efficiency values at the resonant frequency show more noticeable variations across these three distinct software tools. CST simulations have determined that the efficiency at the resonance frequencies is 82.69%, 80.377%, and 90.228%, respectively. The resonance frequencies demonstrate the efficiencies of 80.08%, 86.79%, and 92.62% when implemented in the HFSS software. Lastly, in Altair Feko tools, the efficiencies at the resonant frequencies are recorded as 86.55%, 84.31%, and 92.616%. The persistent high efficiencies at all the resonant frequencies indicate the usefulness of the planned microstrip patch antenna. This means that a significant amount of the power provided to the antenna is radiated as EM waves, contributing to improved performance in transmitting or receiving signals.

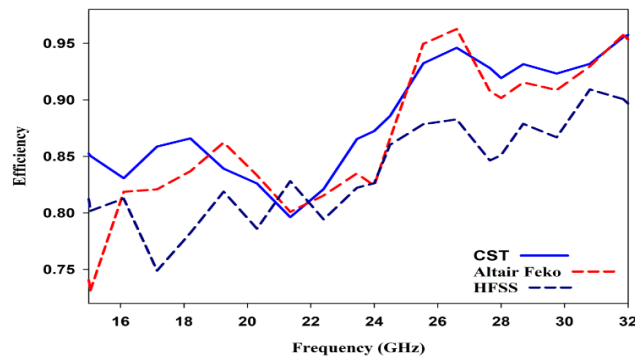


Figure 7. Efficiency of the proposed antenna

4.4. Current distribution

Antennas are instruments used to send or receive EM radiation, such as radio waves, for communication. When an electrical signal stimulates an antenna, it produces a current distribution along its structure. To maximize the performance of antenna devices made to send or receive EM waves, it is essential to comprehend the current distribution [24]. At the antenna's feed and corner edges, the peak surface current is 113.355 A/m as depicted in Figure 8.

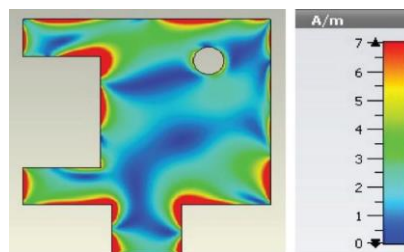


Figure 8. Current distribution of proposed antenna

4.5. Radiation pattern

As the radiation pattern is described on different planes, the letters "XY," "YZ," and "ZX" indicate the antenna orientations and the planes on which the pattern is visible [25]. This electric field, as a function of azimuthal angle (ϕ), is depicted by the E-field radiation pattern. An antenna's H-field radiation pattern describes the changes in the strength and direction of the magnetic field as a function of the polar angle θ [26]. The main lobe magnitude at $\phi = 90^\circ$ is 11 dB V/m, the half-power beam width (HPBW) is 39.3 degrees, and the primary lobe magnitude of the E-field is 21.4 dBV/m at $\phi = 0^\circ$, all calculated at an angular beam width of 39.3 degrees at 3 dB. HPBW of the H-field is 16.6 degrees, and the primary lobe magnitude is -39.5 dB A/m when $\theta = 90$ degrees as presented in Figure 9.

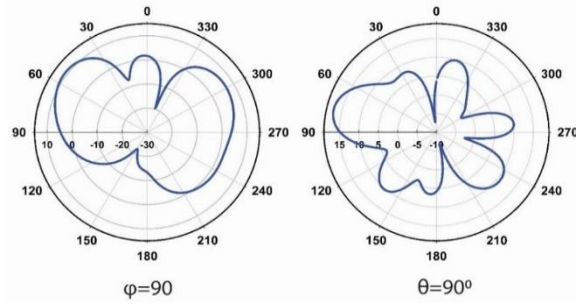


Figure 9. Radiation pattern of the antenna

5. ANN-BASED ANALYSIS OF THE PROPOSED ANTENNA

An ANN model can be trained with data on antenna parameters and their corresponding performance characteristics [27]. The first stage in training an ANN to predict antenna parameters is to collect a dataset of input-output pairs that characterize the relationship between the input parameters and their corresponding output parameters [28]. The parameters of the input, hidden, and output layers of the neural network are presented in the form of a block diagram shown in Figure 10. The network depicted in the picture has 10 hidden layer neurons, 7 inputs, and 2 outputs. Seven inputs, including the ground of the length, the length of the patch, width of the patch, the width of the ground plane, the height of the substrate, the length of the substrate, and the width of the substrate, are combined with two outputs, which are efficiency and gain [29]. Following ANN training with 221 samples, the proportions of training and test data are calculated as depicted in Figure 11.

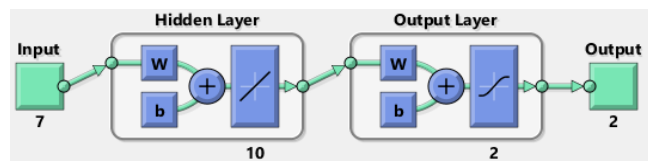


Figure 10. Neural network’s input, latency, and output layers’ parameters

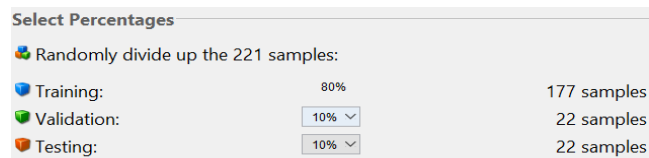


Figure 11. Estimation of training proportions

For this ANN implementation, we opted to use the “Levenberg-Marquardt” (LM) algorithm for training. Figure 12 displays the mean squared error (MSE) and correlation coefficient (R^2) for the training [30], validation, and test values produced by the ANN application. Training yielded an MSE of only 1.5×10^{-3} and $R^2=0.996284$, therefore the accuracy is quite good. When training ANN applications, a value between 80% and 90% is preferred. The confidence interval for the estimated data in this probe is very close to 99 percent as depicted in Figure 13.

Results			
	Samples	MSE	R
Training:	177	1.50162e-3	9.99624e-1
Validation:	22	1.05062e-3	9.99743e-1
Testing:	22	1.51048e-3	9.99652e-1

Figure 12. Training, validation, and testing samples, MSE, and R^2

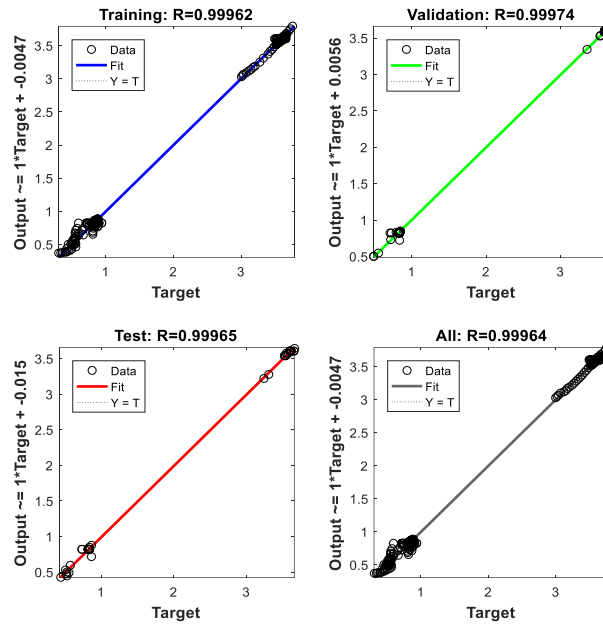


Figure 13. Correlation of efficiency value predicted by ANN

Figures 14 and 15 shows a comparison between the predicted efficiency and gain using ANN and the simulated efficiency and gain. The results of ANN diverge just a little from what was predicted [31]. A near-zero error rate allowed for very accurate prediction of most of the test samples. As demonstrated in Figure 14, the results of the simulation and the prediction regarding efficiency are consistent with one another. On the other hand, Figure 15 depicts the prediction regarding gain.

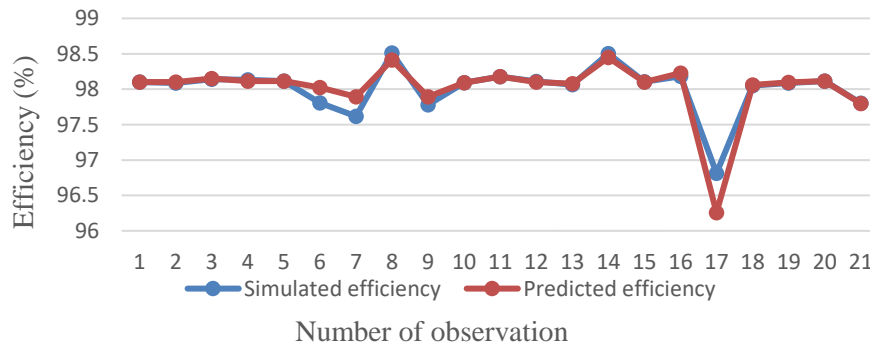


Figure 14. Simulated vs predicted efficiency

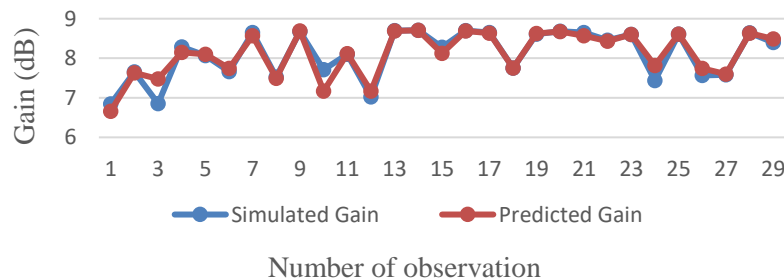


Figure 15. Simulated vs predicted gain using ANN

6. CONCLUSION

This article presents our findings on utilizing an ANN technique to improve the performance of microstrip patch antennas operating at the Ku band. The focus is on enhancing the antenna's capabilities for indoor-outdoor applications and 5G technology. This article discusses many ways, including simulation using software like HFSS and Altair Feko to evaluate the suitability of an antenna. The antenna is constructed using a Rogers RT 5880 substrate. The proposed antenna is small and has a maximum gain of approximately 8 dB and a maximum efficiency of approximately 90%. The evaluation of ANN models can be conducted by utilizing the R-squared coefficient (99%), the mean square error (MSE) which is approximately 0.0015, the ANN models exhibit the minimum error and highest accuracy in predicting gain and efficiency. The suggested antenna has strong suitability for the targeted Ku band, indoor, outdoor, and 5G applications, as evidenced by the simulated results obtained by CST, HFSS, and Altair Feko in conjunction with the measured and predicted outcomes achieved through ANN.

ACKNOWLEDGEMENT

The author expresses gratitude to the Faculty of Graduate Studies and the Department of Electrical and Electronic Engineering of Daffodil International University, Bangladesh, for their cooperation.




REFERENCES

- [1] B. Kaur *et al.*, "Internet of Things (IoT) security dataset evolution: Challenges and future directions," *Internet of Things*, vol. 22, p. 100780, Jul. 2023, doi: 10.1016/j.iot.2023.100780.
- [2] M. I. Jahan, M. R. I. Faruque, and Md. B. Hossain, "An X-shaped triple split ring resonator-based metamaterial perfect absorber with quad-band incident and polarization angle insensitivity for C, X, and Ku band applications," *Journal of Magnetism and Magnetic Materials*, vol. 580, p. 170940, Aug. 2023, doi: 10.1016/j.jmmm.2023.170940.
- [3] S. P. Lavadiya *et al.*, "Low profile multiband microstrip patch antenna with frequency reconfigurable feature using PIN diode for S, C, X, and Ku band applications," *Int. J. Communication*, vol. 35, no. 9, p. e5141, Jun. 2022, doi: 10.1002/dac.5141.
- [4] J. M. Jornet, E. W. Knightly, and D. M. Mittleman, "Wireless communications sensing and security above 100 GHz," *Nat Commun*, vol. 14, no. 1, p. 841, Feb. 2023, doi: 10.1038/s41467-023-36621-x.
- [5] X. Xie, L. Zhang, C. Mao, Y. He, and S. Gao, "High-gain wideband circularly polarised mm-wave antenna with highly symmetrical radiation patterns," *IET Microwaves Antenna & Prop.*, vol. 16, no. 15, pp. 911–918, Dec. 2022, doi: 10.1049/mia.2.12305.
- [6] R. H. Elabd and A. J. A. Al-Gburi, "SAR assessment of miniaturized wideband MIMO antenna structure for millimeter wave 5G smartphones," *Microelectronic Engineering*, vol. 282, p. 112098, Oct. 2023, doi: 10.1016/j.mee.2023.112098.
- [7] Z. Hassan *et al.*, "Spectrum Sharing of the 12 GHz Band with Two-Way Terrestrial 5G Mobile Services: Motivations, Challenges, and Research Road Map," *IEEE Commun. Mag.*, vol. 61, no. 7, pp. 53–59, Jul. 2023, doi: 10.1109/MCOM.007.2200699.
- [8] I. U. Din *et al.*, "Frequency-Selective Surface-Based MIMO Antenna Array for 5G Millimeter-Wave Applications," *Sensors*, vol. 23, no. 15, p. 7009, Aug. 2023, doi: 10.3390/s23157009.
- [9] Md. A. Haque, M. A. Zakariya, L. C. Paul, D. Nath, P. Biswas, and R. Azim, "Analysis of Slotted E-shaped Microstrip Patch Antenna for Ku Band Applications," in *2021 IEEE 15th Malaysia Int. Conf. on Commun.*, 2021, pp. 98–101, doi: 10.1109/MICC53484.2021.9642100.
- [10] S. Rahman *et al.*, "Nature Inspired MIMO Antenna System for Future mmWave Technologies," *Micromachines*, vol. 11, no. 12, p. 1083, Dec. 2020, doi: 10.3390/mi11121083.
- [11] M. Al-Tamimi and R. H. Thaher, "Design of New Compound Reconfigurable Microstrip Antenna for C And Ku Bands Applications," *jeasd*, vol. 27, no. 2, pp. 196–203, Mar. 2023, doi: 10.31272/jeasd.27.2.4.
- [12] J. V. Ayyappan, M. Arulappan, B. A. D. Raj, and S. S. Nadar, "Tri-band Dual Substrate Aperture Coupled Microstrip Antenna for C, X, and Ku Band Applications," *JHCT*, vol. 01, no. 01, pp. 01–11, Jan. 2023, doi: 10.58399/GTMX8376.
- [13] T. Liang, Z. Wang, and Y. Dong, "A Circularly Polarized SIW Slot Antenna Based on High-Order Dual-Mode Cavity," *Antennas Wirel. Propag. Lett.*, vol. 19, no. 3, pp. 388–392, Mar. 2020, doi: 10.1109/LAWP.2020.2972115.
- [14] M.-A. Chung, K.-C. Tseng, and I.-P. Meiy, "Antennas in the Internet of Vehicles: Application for X Band and Ku Band in Low-Earth-Orbiting Satellites," *Vehicles*, vol. 5, no. 1, pp. 55–74, Jan. 2023, doi: 10.3390/vehicles5010004.
- [15] M. Khalid *et al.*, "4-Port MIMO Antenna with Defected Ground Structure for 5G Millimeter Wave Applications," *Electronics*, vol. 9, no. 1, p. 71, Jan. 2020, doi: 10.3390/electronics9010071.
- [16] R. Przesmycki, M. Bugaj, and L. Nowosielski, "Broadband Microstrip Antenna for 5G Wireless Systems Operating at 28 GHz," *Electronics*, vol. 10, no. 1, p. 1, Dec. 2020, doi: 10.3390/electronics10010001.
- [17] A. A. Megahed, E. H. Abdelhay, M. Abdelazim, and H. Y. M. Soliman, "5G millimeter wave wideband MIMO antenna arrays with high isolation," *J Wireless Com Network*, vol. 2023, no. 1, p. 61, Jul. 2023, doi: 10.1186/s13638-023-02267-y.
- [18] A. Ejaz *et al.*, "A High Performance All-Textile Wearable Antenna for Wristband Application," *Micromachines*, vol. 14, no. 6, p. 1169, May 2023, doi: 10.3390/mi14061169.
- [19] J. Monica and P. Jothilakshmi, "A Design of Bandwidth-Enhanced Conformal Antenna for Aircraft Applications," *IETE Journal of Research*, vol. 69, no. 1, pp. 447–459, Jan. 2023, doi: 10.1080/03772063.2020.1829507.
- [20] S. Maity, T. Tewary, S. Mukherjee, A. Roy, P. P. Sarkar, and S. Bhunia, "Super wideband high gain hybrid microstrip patch antenna," *AEU-International Journal of Electronics and Communications*, vol. 153, p. 154264, Aug. 2022, doi: 10.1016/j.aeue.2022.154264.
- [21] V. Mandrić, S. Rupčić, S. Rimac-Drlje, and I. Baxhaku, "Influence of Dielectric Plate Parameters on the Reflection Coefficient of a Planar Aperture Antenna," *Applied Sciences*, vol. 13, no. 4, p. 2544, Feb. 2023, doi: 10.3390/app13042544.
- [22] L. C. Paul, M. A. Haque, M. A. Haque, M. M. U. Rashid, M. F. Islam, and M. M. Rahman, "Design a slotted metamaterial microstrip patch antenna by creating three dual isosceles triangular slots on the patch and bandwidth enhancement," in *2017 3rd International Conference on Electrical Information and Communication Technology (EICT)*, Dec. 2017, pp. 1–6, doi: 10.1109/EICT.2017.8275143.
- [23] I. Ahmad, W. Tan, Q. Ali, and H. Sun, "Latest Performance Improvement Strategies and Techniques Used in 5G Antenna Designing Technology, a Comprehensive Study," *Micromachines*, vol. 13, no. 5, p. 717, Apr. 2022, doi: 10.3390/mi13050717.
- [24] N. Bisht, P. K. Malik, S. Das, T. Islam, S. Asha, and M. Alathbah, "Design of a Modified MIMO Antenna Based on Tweaked Spherical Fractal Geometry for 5G NR Band N258 (24.25–27.25 GHz) Appl.," *Fractal Fract*, vol. 7, no. 10, p. 718, 2023, doi: 10.3390/fractal7100718.




- [25] L. C. Paul, M. S. Akhter, M. A. Haque, M. R. Islam, M. F. Islam, and M. M. Rahman, "Design and analysis of four elements E, H and combined E-H shaped microstrip patch array antenna for wireless applications," in *2017 3rd International Conference on Electrical Information and Communication Technology (EICT)*, Khulna: IEEE, Dec. 2017, pp. 1–6, doi: 10.1109/EICT.2017.8275141.
- [26] A. Boukarkar, S. Rachdi, M. M. Amine, B. Sami, and A. B. Khalil, "A compact four states radiation-pattern reconfigurable monopole antenna for Sub-6 GHz IoT applications," *AEU-International Journal of Electronics and Communications*, vol. 158, p. 154467, Jan. 2023, doi: 10.1016/j.aeue.2022.154467.
- [27] M. Moshaghzadeh, A. Bakhtiari, E. Izadpanahi, and P. Mardanpour, "Artificial Neural Network for the prediction of fatigue life of a flexible foldable origami antenna with Kresling pattern," *Thin-Walled Structures*, vol. 174, p. 109160, May 2022, doi: 10.1016/j.tws.2022.109160.
- [28] M. Kurucan, M. Özbaltan, Z. Yetgin, and A. Alkaya, "Applications of artificial neural network based battery management systems: A literature review," *Renewable and Sustainable Energy Reviews*, vol. 192, p. 114262, Mar. 2024, doi: 10.1016/j.rser.2023.114262.
- [29] E. T. Sayed, H. Rezk, M. A. Abdelkareem, and A. G. Olabi, "Artificial neural network based modelling and optimization of microalgae microbial fuel cell," *International Journal of Hydrogen Energy*, vol. 52, pp. 1015–1025, Jan. 2024, doi: 10.1016/j.ijhydene.2022.12.081.
- [30] S. N. Mughal, Y. R. Sood, and R. K. Jarial, "Techno-economic assessment of photovoltaics by predicting daily global solar radiations using hybrid ANN-PSO model," *Energy Syst*, Feb. 2024, doi: 10.1007/s12667-023-00646-4.
- [31] O. Singh, M. R. Bharamagoudra, H. Gupta, A. K. Dwivedi, P. Ranjan, and A. Sharma, "Microstrip line fed dielectric resonator antenna optimization using machine learning algorithms," *Sādhanā*, vol. 47, no. 4, p. 226, Nov. 2022, doi: 10.1007/s12046-022-01989-x.

BIOGRAPHIES OF AUTHORS






Md. Kawsar Ahmed    is currently pursuing his studies in the field of Electrical and Electronic Engineering at Daffodil International University. He successfully finished his Higher Secondary education at Agricultural University College, Mymensingh. He is presently employed as a student associate at Daffodil International University (DIU) in Bangladesh. The areas of his research focus encompassed microstrip patch antennas, terahertz antennas, and applications related to 4G and 5G technologies. He can be contacted at email: kawsar33-1241@diu.edu.bd.






Kamal Hossain Nahin    is currently pursuing a degree in Electrical and Electronic Engineering at Daffodil International University. His educational journey commenced at Ishwardi Govt College for Higher Secondary Certificate (HSC) and earlier at Maniknagar High School for Secondary School Certificate (SSC). Embarking on a journey as a budding researcher in the communication field, he is passionately immersed in exploring the realms of wireless communication. His focus lies in delving into the intricacies of wireless communication, particularly exploring microstrip patch antennas, terahertz antennas, and their potential applications in the future realms of 5G and 6G technologies. He can be contacted at email: kamal33-1242@diu.edu.bd.






Md. Sharif Ahammed    is a student of Daffodil International University and pursuing a B.Sc. in the Electrical and Electronics Department. He passed from Government Bangabandhu college with a higher secondary. Microstrip patch antenna, terahertz antenna, and 5G application are some of his research interests. He can be contacted at email: sharif33-1152@diu.edu.bd.




Md. Ashraf Haque    is doing Ph.D. at the Department of Electrical and Electronic Engineering, Universiti Teknologi PETRONAS, Malaysia, He got his B.Sc. in Electronics and Electronic Engineering (EEE) from Bangladesh's Rajshahi University of Engineering and Technology (RUET) and his M.Sc. in the same field from Bangladesh's Islamic University of Technology (IUT). He is currently on leave from Daffodil International University (DIU) in Bangladesh. His research interest includes microstrip patch antenna, sub 6 5G application, and supervised regression model machine learning on antenna design. He can be contacted at email: limon.ashraf@gmail.com.






Narinderjit Singh Sawaran Singh    is an Associate Professor in INTI International University, Malaysia. He graduated from the Universiti Teknologi PETRONAS (UTP) in 2016 with Ph.D. in Electrical and Electronic Engineering specialized in probabilistic methods for fault tolerant computing. Currently, he is appointed as the research cluster head for computational mathematics, technology and optimization which focuses on the areas like pattern recognition and symbolic computations, game theory, mathematical artificial intelligence, parallel computing, expert systems and artificial intelligence, quality software, information technology, exploratory data analysis, optimization algorithms, stochastic methods, data modelling, and computational intelligence-swarm intelligence. He can be contacted at email: narinderjits.sawaran@newinti.edu.my.






Redwan Al Mahmud Asad Ananta    has accomplished his undergraduate studies in the Field of Electrical and Electronics at Daffodil International University. He completed his higher secondary education at Adamjee Cantonment College. His research focus encompasses wireless communication, specifically microstrip patch antenna, terahertz antenna, and 5G, and 6G applications. He can be contacted at email: redwan33-1145@diu.edu.bd.






Jamal Hossain Nirob    is a student in the Department of Electrical and Electronic Engineering (EEE) at Daffodil International University. His educational journey began at Maniknagar High School, where he successfully completed his Secondary School Certificate (SSC). Following that, he pursued higher studies at Ishwardi Government College, obtaining his Higher Secondary Certificate (HSC). With a strong enthusiasm for expanding communication technology, Jamal has focused his research on wireless communication, specifically on microstrip patch antennas, terahertz antennas, and applications of 5G and 6G. He can be contacted at email: jamal33-1243@diu.edu.bd.



Mirajul Islam    is a distinguished Computer Science and Engineering graduate from Daffodil International University, Dhaka, Bangladesh, is a dedicated researcher with a profound impact on academia. Specializing in machine learning, deep learning, cybersecurity, natural language processing, image processing, computer vision, and more, his 8+ Scopus-indexed journals and 10+ Scopus-indexed conference publications attest to his significant contributions. His research spans diverse technological domains, showcasing a commitment to pushing the boundaries of knowledge. His work not only enriches academic discourse but also holds practical implications, contributing to advancements in technology. His trajectory as a thought leader and innovator positions him as a beacon in the dynamic realm of research and data science, inspiring others to explore the intersections of technology and drive meaningful change. He can be contacted at email: merajul15-9627@diu.edu.bd.



Liton Chandra Paul (SMIEEE)    successfully finished his Master's degree in Electrical and Electronic Engineering and Bachelor's degree in Electronics and Telecommunication Engineering in 2012 and 2015, respectively. Throughout his time as a student, he has made generous contributions to numerous non-profitable social welfare organizations. He also serves as a reviewer for many int'l reputed conferences and journals of different reputed publishers, including IEEE, Springer Nature, Elsevier, Wiley, Cambridge University Press, IET, Hindawi, MDPI, Taylor & Francis, etc. He has affiliations with different national and int'l professional bodies like the Institute of Engineers Bangladesh (IEB) and the Institute of Electrical and Electronics Engineers (IEEE), including IEEE-APS, IEEE-MTTS, IEEE-ComSoc, IEEE-SPS, IEEE-WIE, etc. His research interests are RFIC, MIMO, Machine learning, bio-electromagnetics, microwave technology, antennas, phased arrays, mmWave, metamaterials, Absorber, metasurfaces, wireless sensors, etc. He can be contacted at email: litonpaulete@gmail.com.